Impact of a local *CP*-odd domain in hot QCD on the axionic domain-wall interpretation of NANOGrav 15-year data

Linlin Huang,[*] Yuanyuan Wang,[†] He-Xu Zhang,[‡] and Shinya Matsuzaki[§]

Center for Theoretical Physics and College of Physics, Jilin University,
Changchun 130012, China

Hiroyuki Ishida[‖]

Center for Liberal Arts and Sciences, Toyama Prefectural University,
Toyama 939-0398, Japan

Mamiya Kawaguchi[¶]

School of Nuclear Science and Technology, University of Chinese Academy of Sciences,
Beijing 100049, China

Akio Tomiya[**]

Department of Information Technology, International Professional University of Technology in Osaka,
3-3-1 Umeda, Kita-Ku, Osaka 530-0001, Japan

We argue that the axionic domain-wall with a QCD bias may be incompatible with the NANOGrav 15-year data on a stochastic gravitational wave (GW) background, when the domain wall network collapses in the hot-quantum chromodynamics (QCD) induced local *CP*-odd domain. This is due to the drastic suppression of the QCD bias set by the QCD topological susceptibility in the presence of the *CP*-odd domain with nonzero θ parameter of order one which the QCD sphaleron could generate. We quantify the effect on the GW signals by working on a low-energy effective model of Nambu-Jona-Lasinio type in the mean field approximation. We find that only at $\theta = \pi$, the QCD bias tends to get significantly large enough due to the criticality of the thermal *CP* restoration, which would, however, give too big signal strengths to be consistent with the NANOGrav 15-year data and would also be subject to the strength of the phase transition at the criticality.

I. INTRODUCTION

The observation of a stochastic GW background has recently reported from the NANOGrav pulsar timing array collaboration in 15 years of data [1,2]. Possible origins of the detected nano-Hz peak frequency in a view of particle physics have been investigated also by the NANOGrav

[*]huangll22@mails.jlu.edu.cn
[†]yuanyuanw23@jlu.edu.cn
[‡]hxzhang18@163.com
[§]synya@jlu.edu.cn
[‖]ishidah@pu-toyama.ac.jp
[¶]mamiya@ucas.ac.cn
[**]akio@yukawa.kyoto-u.ac.jp

collaboration [3]. Other recent pulsar timing array (PTA) data, such as those from the European PTA (EPTA) [4–6], Parkes PTA (PPTA) [7,8], and Chinese PTA (CPTA) [9] have also supported the presence of consistent nano-Hz stochastic GWs. Thus this nano-Hz GW evidence might provide us with a hint on the new aspect of the thermal history of the universe in terms of beyond the standard model of particle physics.

Among the new-physics candidate interpretations, the axionlike particle (ALP)-domain wall annihilation triggered by a QCD-induced bias has been considered as an attractive model [10–17], which can naturally be realized in the QCD-phase transition epoch at the temperature $T \sim \mathcal{O}(100)$ MeV consistent with the produced peak frequency of nano Hz [3]. The QCD-induced bias is supplied by the topological susceptibility $\chi_{\rm top}$, and its T-dependence and the value at $T = 0$ have already been measured in a lattice simulation at the physical point for quark masses with the continuum limit is properly taken [18]. This is how

the ALP-domain wall prediction gets definite and unambiguous except the domain-wall network formulation and annihilation analysis, even though the system that the ALP acts in is nonperturbative QCD.

However, the thermal history of the QCD phase transition epoch may not be so simple: a local *CP*-odd domain may be created in hot QCD plasma due to the presence of the QCD sphaleron [19,20], so that the QCD vacuum characterized by the strong *CP* phase θ and its fluctuation (in the spatial-homogeneous direction) gets significantly sizable [21–23] within the QCD timescale [24–27].[1] Though θ should be tiny enough ($< 10^{-10}$) at present, nonzero θ contribution to the QCD bias χ_{top} may be non-negligible when the ALP domain wall starts to collapse in the QCD phase transition epoch. This is irrespective to whether or not the ALP acts as the QCD axion which relaxes the θ to zero at present.

In this paper, we argue that the ALP-domain wall with the QCD bias becomes incompatible with the NANOGrav 15-year data on a stochastic GW background, when the domain wall network collapses in the hot-QCD induced local-*CP* odd domain. This happens due to the drastic suppression of the QCD bias set by the QCD topological susceptibility in the presence of the *CP*-odd domain with nonzero θ parameter of order one which the QCD sphaleron could generate.

This paper is structured as follows. We first make a generic argument. It is based only on the anomalous Ward-Takahashi identities in QCD and the mixing structure between the scalar quark condensate ($\langle \bar{q}q \rangle$) and pseudo-scalar quark condensate ($\langle \bar{q}i\gamma_5 q \rangle$) bilinear operators via the $U(1)$ axial transformation with nonzero θ. χ_{top} is shown to generically get small when θ takes the value of order one, because of the dramatic suppression of the scalar quark condensate at any temperature.

We next implement this suppression effect into the produced GW signals by working on a low-energy effective model of Nambu-Jona-Lasinio (NJL) type in the mean field approximation (MFA) and the random phase approximation (RPA). In accord with the generic argument, χ_{top} as well as the scalar quark condensate get highly suppressed

---

[1]The QCD sphaleron transition rate is not suppressed by the thermal effect in contrast to the QCD instanton's one [25–27]. The topological charge fluctuation (within the QCD timescale $= \mathcal{O}(1\text{-}10)$ fm), $\Delta q_{\text{top}}(t) = \int^t dt' \, d\vec{x}^3 Q_{\text{top}}(t', \vec{x})$, will be nonvanishing. This implies that the corresponding source $\theta(x)$ in the generating functional Z_{QCD} needs to be (at least) time-dependent and fluctuate: $\delta Z_{\text{QCD}} / \delta \Delta \theta(t) \sim q_{\text{top}}(t) \neq 0$. The time and/or thermal average of $\Delta \theta(t)$ thus acts as what we call the theta parameter in the QCD thermal plasma, which namely means $\theta \equiv \Delta \theta(t)$ in there. See also, e.g., the literature [28,29]. Besides, the time fluctuation $\partial_t \theta(t)$, to be referred to as the chiral chemical potential [21–23,28,29], will be significant as well when the nonconservation law of the $U(1)$ axial symmetry is addressed. See also Summary and Discussions.

when $\theta = \mathcal{O}(1)$, instead, the pseudoscalar condensate as the *CP*/axial partner develops.

We also find that only at $\theta = \pi$, the QCD bias tends to get significantly large enough due to the criticality of the thermal *CP* restoration of the second order, which is signaled when the pseudoscalar condensate reaches zero. This, however, gives too big signal strengths to be consistent with the NANOGrav 15-year data. Going beyond the MFA or other types of effective models could yield a different strength of the phase transition at the criticality. In summary of the present paper, we also briefly address the outlook along this possibility and the prospective impact on the QCD bias for the ALP-domain wall annihilation in light of nano Hz GW signals.

II. GENERAL ARGUMENT

We begin with presenting a general consequence on the suppression of χ_{top} when $\theta = \mathcal{O}(1)$. First of all, we note that the anomalous $U(1)$ axial transformation ($q \to e^{-i\gamma_5 \frac{\theta}{4}} q \equiv q'$) can make the θ dependence in QCD present only in the quark mass term. In two-flavor QCD, for simplicity, the quark mass term then takes the form

$$\sum_{q=u,d} \left[m \cos \frac{\theta}{2} (\bar{q}'q') + m \sin \frac{\theta}{2} (\bar{q}'i\gamma_5 q') \right], \qquad (1)$$

where the primed quark bilinear fields are related to the original ones via the orthogonal rotation,

$$\begin{pmatrix} \bar{q}q \\ \bar{q}i\gamma_5 q \end{pmatrix} = \begin{pmatrix} \cos \frac{\theta}{2} & \sin \frac{\theta}{2} \\ -\sin \frac{\theta}{2} & \cos \frac{\theta}{2} \end{pmatrix} \begin{pmatrix} \bar{q}'q' \\ \bar{q}'i\gamma_5 q' \end{pmatrix}. \qquad (2)$$

The scalar condensate $\langle \bar{q}q \rangle$ thus mixes with the pseudo-scalar one $\langle \bar{q}i\gamma_5 q \rangle$ by nonzero θ.

χ_{top} is given as the functional derivative of the generating functional of QCD twice with respect to θ evaluated at $\theta \neq 0$. Taking into account the quark mass term in Eq. (1) we thus get

$$i\chi_{\text{top}}(T, \theta) = \int_T d^4x \langle Q_{\text{top}}(x) Q_{\text{top}}(0) \rangle_\theta,$$

$$Q_{\text{top}}(x) = \frac{g_s^2}{32\pi^2} G_{\mu\nu} \tilde{G}^{\mu\nu}, \qquad (3)$$

where Q_{top} denotes the topological charge with the QCD gauge coupling g_s and the (dual) field strength $G_{\mu\nu}$ ($\tilde{G}_{\mu\nu} \equiv \frac{\epsilon_{\mu\nu\rho\sigma}}{2} G^{\rho\sigma}$); $\int_T d^4x \equiv \int_0^{1/T} d\tau \int d^3x$ with the imaginary time $\tau = ix_0$; the subscript "θ" attached on the vacuum (thermodynamic ground) states stands for the implicit θ parameter dependence. Following the procedure in the literature [30–32] χ_{top} in two-flavor QCD is expressed in terms of the original-basis fields as

$$\chi_{\text{top}}(T,\theta) = -\frac{1}{4}\left[m\sum_{q=u,d}\langle\bar{q}q\rangle_{\theta,T} + im^2\chi_\eta(T,\theta)\right], \quad (4)$$

where we have taken the isospin symmetric mass for up (u) and down (d) quarks, and

$$\chi_\eta(T,\theta) = \int_T d^4x \sum_{q=u,d}\langle(\bar{q}(0)i\gamma_5 q(0))(\bar{q}(x)i\gamma_5 q(x))\rangle_\theta, \quad (5)$$

which is $\sim\frac{\partial}{\partial T}\sum_{q=u,d}\langle\bar{q}i\gamma_5 q\rangle_{\theta,T}$. Since the quark mass is perturbatively small enough and $\langle\bar{q}q\rangle$ develops a nonzero value at the normal QCD vacuum with $\theta = 0$, the chiral perturbation conventionally works well for χ_{top}, so that the $\langle\bar{q}q\rangle$ term will dominate over the χ_η term, to saturate the measured χ_{top} value $\simeq(75.6\text{ MeV})^4$, i.e.,

$$|\chi_{\text{top}}(T,\theta=0)| \approx \frac{1}{4}m\sum_{q=u,d}|\langle\bar{q}q\rangle_{\theta=0,T}| \simeq (75.6\text{ MeV})^4. \quad (6)$$

This is sort of the well-known formula called the Leutwyler-Smiluga formula [33], and this feature has also been observed in chiral effective model approaches at any T [30–32,34]. When $\theta \neq 0$, however, the value of $\langle\bar{q}q\rangle$ will be shared with the pseudoscalar condensate $\langle\bar{q}i\gamma_5 q\rangle$ through Eq. (2), so that $\langle\bar{q}q\rangle$ term in χ_{top} of Eq. (4) gets small, to be as small as or smaller than the χ_η term, as θ gets sizable. Thus, we expect the dramatic suppression of χ_{top} at a sizable θ^2:

$$|\chi_{\text{top}}(T,\theta=\mathcal{O}(1))| \approx \frac{1}{4}m^2|\chi_\eta(T,\theta)| \ll |\chi_{\text{top}}(T,\theta=0)|. \quad (7)$$

This trend will be seen for any T and χ_{top} would simply get smaller and smaller as T increases unless a sharp phase transition in χ_η shows up at higher T. Thus, the magnitude of the QCD-induced bias for the ALP domain wall annihilation, controlled by χ_{top}, is expected to become dramatically small in the local *CP*-odd domain created in hot QCD.

Below we will explicitly support this claim based on an NJL with nonzero θ.

---

[2]Even when the strange quark contributions are incorporated in χ_{top}, the form of Eq. (4) is intact, as has been discussed in the literature [30–32,34] and also reviewed in Appendix A, hence χ_{top} can be evaluated only via the lightest quark condensate and χ_η, in which the strange-quark loop contributions are implicitly incorporated. Thus the lightest quark condensate term ($\sum_{q=u,d}\langle\bar{q}q\rangle$) in $|\chi_{\text{top}}(T,\theta=\mathcal{O}(1))|$ still persists being suppressed due to the sizable *CP* violation, while the χ_η term keeps sizable with the large *CP* violation, where the *CP*-violating strange quark contribution almost decouples simply because of its heaviness (see also Summary and Discussions). Therefore, the inequality in Eq. (7) holds even in the case of three-flavor QCD.

III. NJL EVALUATION OF χ_{top} AND ALP DOMAIN WALL ENERGY DENSITY WITH NONZERO θ

Since lattice data on $\chi_{\text{top}}(T,\theta)$ with $\theta \neq 0$ have not yet been available,[3] we employ a low-energy chiral effective model, an NJL model, which matches with the underlying QCD via the consistent anomalous Ward-Takahashi identities associated with the chiral $SU(2)$ and $U(1)$ axial symmetry breaking. The investigation of QCD with nonzero θ has so far been carried out based on several chiral effective models [16,35–49] and also the recently developed 't Hooft-anomaly matching method [50,51] extended from the original idea [52,53], so as to clarify the nature of the thermal chiral and strong *CP* phase transitions when $\theta = \pi$. Nevertheless, the T and θ dependence on χ_{top} has never been addressed except Ref. [46]. In the reference χ_{top} was computed based on the same NJL model as what we will work on below, however, consistency with the anomalous chiral Ward-Takahashi identities was not manifest, which is to be refined in the present study. We leave all the technical details in Appendices A and B and shall only give the results relevant to the discussion of the nano Hz GW signals.

The dependence of T and θ on χ_{top} is plotted in Fig. 1. The present model yields $|\chi_{\text{top}}^{1/4}(T=0,\theta=0)| \simeq 77.5$ MeV, which is in good agreement with the lattice estimate, $\chi_{\text{top}}^{1/4}(T=0,\theta=0) \simeq 75.6$ MeV [18]. As seen from the left panel of the figure, χ_{top} prominently gets smaller when $\theta \gtrsim 0.5\pi$, which is due to the suppression of $\langle\bar{q}q\rangle$ (as shown in Appendix B), instead $\langle\bar{q}i\gamma_5 q\rangle$ gets greater than $\langle\bar{q}q\rangle$, as was expected from the generic argument in Eq. (7). We also note from Appendix B that the chiral phase transition goes like crossover for any θ, whereas the *CP* phase transition is of the second order type at $\theta = \pi$ (see Fig. 1), which is also manifested as a spike structure of χ_{top}. In particular, the *CP* symmetry is restored at the criticality ($T \simeq 221$ MeV) in accordance with the literature [40,42,43].

We assume that an ALP has already been present before the QCD phase transition epoch as in the literature [10–17] and developed the potential having the shift symmetry, $a \to a + 2\pi f_a$ with n_{DW} being integer:

$$V_0(a) = \frac{m_a^2 f_a^2}{n_{\text{DW}}^2}\left(1 - \cos\left(n_{\text{DW}}\frac{a}{f_a}\right)\right), \quad (8)$$

where m_a and f_a are the ALP mass and decay constant, respectively. Then a domain wall profile exists as a soliton solution, which sweeps between the adjacent vacua, where n_{DW} in V_0 above corresponds to the domain wall number. As the universe cools down to the QCD scale, assuming existence of the ALP coupling to gluon fields, the ALP develops another potential via the $U(1)$ axial anomaly,

---

[3]For more on the current status and future prospects, see also Summary and Discussions.

$$V_{QCD}(a) = -\chi_{top}(T, \theta) \cos\left(n\frac{a}{f_a} + \theta\right), \qquad (9)$$

which explicitly breaks the original shift symmetry, where n is some factor related to and highly depending on the Peccei-Quinn charges of quarks. The original ALP vacuum-potential energy $\sim m_a^2 f_a^2$ is assumed to be $\gtrsim |\chi_{top}|$. Thus the domain wall configuration, which is supported by the original shift symmetry, becomes unstable in the total ALP potential $V_{total} = V_0 + V_{QCD}$:

$$V_{total}(a) = \frac{m_a^2 f_a^2}{n_{DW}^2}\left(1 - \cos\left(n_{DW}\frac{a}{f_a}\right)\right)$$
$$+ \chi_{top}\left(\cos\theta - \cos\left(n\frac{a}{f_a} + \theta\right)\right), \qquad (10)$$

with the normalization $V_{total}(a = 0) = 0$. Meanwhile, the domain wall network (with $n_{DW} \geq 2$) starts to collapse and release the latent heat into the universe. Here, $V_{QCD}(a)$ plays the role of what is called the bias, ΔV. The released energy density can be evaluated by the vacuum energy at the original vacua $a = n_{DW}\pi f_a$. For instance, when $n_{DW} = 2$, the original vacuum at $a/f_a = \pi$ gets the energy shift by $|V_{total}(a/f_a = \pi)| = |V_0 - V_{QCD}|_{a/f_a = \pi}$:

$$|V_0 - V_{QCD}|_{a/f_a = \pi} = |\chi_{top}(T, \theta)(\cos(n\pi + \theta) - \cos\theta)|$$
$$\sim |\chi_{top}(T, \theta)| \equiv \Delta V(T, \theta). \qquad (11)$$

Thus one may maximally have the released latent heat $\rho_{DW}(T)$

$$\rho_{DW} \sim \Delta V(T, \theta) = |\chi_{top}(T, \theta)|. \qquad (12)$$

Similar discussions have been made in the literature [10–17]. A more precise estimate based on the numerical simulations of the domain wall network suggests $\rho_{DW} \simeq 0.5\Delta V$ [54–57].

The QCD bias $|\chi_{top}|$ generically does not significantly affect the ALP potential when the universe is hotter than the QCD scale of $\mathcal{O}(100)$ MeV, as seen from Fig. 1 and also from the generic formula in Eq. (4). This is essentially due to the correlation of the effective restoration of the chiral $SU(2)$ (via $\langle \bar{q}q \rangle$) and/or $U(1)$ axial symmetry (χ_η) at higher temperatures [See Eq. (4)]. We assume that the ALP-domain wall annihilation takes place at $T = T_*$ by the QCD bias and fully provides the source of the GW.[4] The produced GW power spectrum at the peak frequency is then assessed via the signal strength, free from the domain

---

[4]The ALP domain wall network will completely be decayed never to be left before the expected domain wall-dominated epoch arises. The critical temperature for the domain wall domination is estimated by using the present NJL model and evaluating the condition $\rho_{DW}/\rho_{rad} > 1$, to give $T = T_{dom} \sim 19$ MeV, which is indeed much lower than the QCD scale.

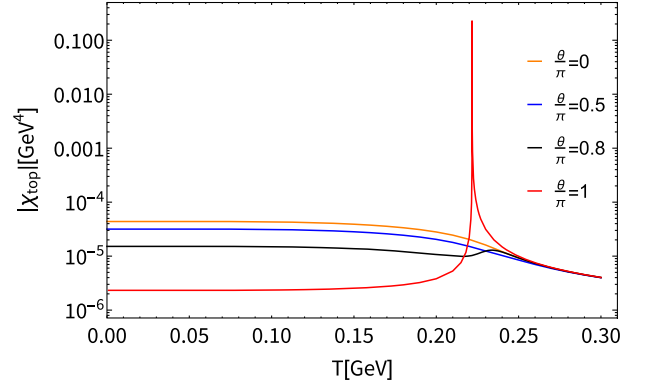FIG. 1. Plot of χ_{top} (in magnitude) computed from the present two-flavor NJL model with nonzero θ.

wall string tension $\sigma_{DW} \sim m_a f_a^2$, by the following signal strength (see, e.g., [17]):

$$\alpha_*(T_*, \theta) = \frac{\rho_{DW}(T_*)}{\rho_{rad}(T_*)} \simeq \frac{0.5\Delta V(T_*, \theta)}{\rho_{rad}(T_*)}$$
$$\simeq 0.15 \times \left(\frac{|\chi_{top}(T_*, \theta)|^{1/4}}{100 \text{ MeV}}\right)^4$$
$$\times \left(\frac{T_*}{100 \text{ MeV}}\right)^{-4}\left(\frac{g_*(T_*)}{10}\right)^{-1}, \qquad (13)$$

where we have used $\rho_{DW} \simeq 0.5\Delta V$ [54–57] and $\rho_{rad}(T) = (\pi^2/30)g_*(T)T^4$. This α_* has been constrained by the NANOGrav 15 yr dataset as a function of T_*. See Fig. 2,
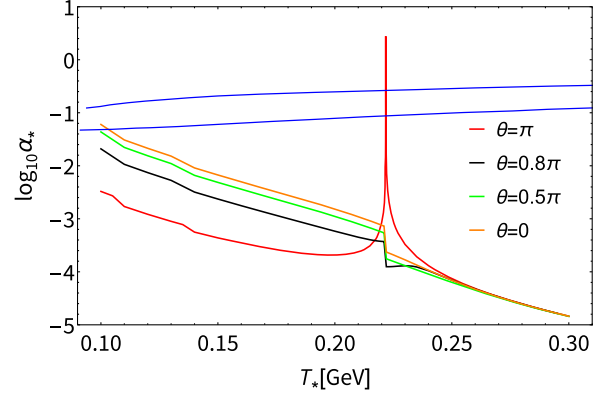

FIG. 2. The contour plot for the signal strength $\alpha_*(\theta)$ in Eq. (13) versus the ALP domain wall annihilation temperature T_* with χ_{top} in Fig. 1 encoded. The 2σ contour from Ref. [3] has also been displayed in blue, and the regimes inside the 2σ contour are thus allowed. α_* in Eq. (13) depends on the effective degrees of freedom $g_*(T)$ around the QCD phase transition epoch, which we have adjusted $g_*(T)$ available in Ref. [58], in such a way that the deconfinement transition happens at the same time as the chiral phase transition in the present NJL model takes place (at $T = 221$ MeV). The wiggles seen around a lower T regime in the model prediction curves have thus been arisen from the thresholds encoded in $g_*(T)$.

showing that the cases with $\theta/\pi \gtrsim 0.5$ are incompatible with the interpretation of the NANOGrav 15-year data at around $T_* = 100$ MeV. This is essentially due to the suppression of the scalar quark condensate as observed in $\chi_{\rm top}$ as shown in Fig. 1. At $\theta = \pi$ onset the criticality (at $T \simeq 221$ MeV), the signal gets dramatically enhanced by the singular spike structure reflecting the second order phase transition of the *CP* symmetry, which is, however, to be too big to interpret the data. This feature is insensitive to the deconfinement phase transition of QCD, which has not yet been incorporated in the figure.

IV. SUMMARY AND DISCUSSIONS

In summary, the ALP domain wall with a QCD bias may be incompatible with the NANOGrav 15-year data on a stochastic GW background, when the domain wall network collapses in the hot-QCD induced local-*CP* odd domain which could allow to have a sizable QCD θ parameter. This is due to the drastic suppression of the QCD bias set by the QCD topological susceptibility, $\chi_{\rm top}$, in the presence of the *CP*-odd domain with $\theta = \mathcal{O}(1)$ (see Eq. (7) and Fig. 1). An explicit model analysis of $\chi_{\rm top}$ with a large θ based on the two-flavor NJL model implies that only at $\theta = \pi$, the QCD bias tends to get significantly large enough due to the criticality of the thermal *CP* restoration. However, this turned out to give too big signal strengths to be consistent with the NANOGrav 15-year data.

In closing, we give several comments on the issues to be pursed in the future.

(i) The presently employed MFA of NJL model does not precisely reproduce the chiral crossover at $\theta = 0$ as has been observed in the lattice simulations. The latter predicts the pseudocritical temperature $T_{\rm pc} \simeq$ 155 MeV [59–63], while the present model yields $T_{\rm pc} \simeq 220$ MeV. This may imply a simple shift of the T-distribution of $\chi_{\rm top}$ in Fig. 1 and also $\alpha_*(\theta)$ toward lower T with lower criticality, say, at $T \sim 160$ MeV. Even in that case, however, the trend of the dramatic suppression of $\chi_{\rm top}$ with $\theta = \mathcal{O}(1)$ should keep manifest for below the shifted criticality ($\sim$160 MeV) and the spike signal associated with the strong *CP* restoration at $\theta = \pi$ will be left at the criticality.

(ii) In Appendix B we have also taken into account a sort of the QCD deconfinement phase transition by extending the NJL model into the Polyakov-loop NJL (PNJL) model [64] (for a recent review, see, e.g., [65]). It turns out that the high suppression of $\chi_{\rm top}$ with $\theta = \mathcal{O}(1)$ is still manifest and the presence of a sharp spike in $\chi_{\rm top}$ at $\theta = \pi$ still persists, in accord with the earlier work [43]. This implies the insensitivity of the deconfinement-confinement transition for the main conclusion addressed in the main text.

(iii) The local *CP*-odd domain would generate not only a large θ, but also the fluctuation of θ in the temporal direction, $\partial_t\theta(t)$, which is identified as the so-called chiral chemical potential (often denoted as μ_5) [21–23]. The μ_5 contribution to the thermal chiral phase transition as well as $\chi_{\rm top}$ has been discussed in Ref. [66] based on a two-flavor NJL model with $\theta = 0$. From the reference we can see that a part of $\chi_{\rm top}$, which only includes the scalar condensate term $\langle \bar{q}q \rangle$ as in Eq. (6) [without the χ_η contribution in Eq. (4)], roughly gets enhanced by about a factor of $(3/2)$ at around $T = \mathcal{O}(100)$ MeV. With $\theta = \mathcal{O}(1)$, the scalar condensate $\langle \bar{q}q \rangle$ generically gets smaller due to the *CP* violation as in the generic argument (Sec. II), which still holds even in the presence of μ_5 because $\mu_5 \sim \partial_t\theta(t)$ does not modify the mixture structure between $\langle \bar{q}q \rangle$ and $\langle \bar{q}i\gamma_5 q \rangle$ as in Eq. (2). Furthermore, the presence of μ_5 as well as nonzero θ does not change the form of all the anomalous chiral Ward-identities as clarified in Appendix A. Hence the high suppression of $\chi_{\rm top}$ would still be seen even with μ_5, so the conclusion as presently claimed would be intact. More precise discussions including the size of the spike at $\theta = \pi$ would be worth pursuing elsewhere.

(iv) The criticality associated with the thermal *CP* restoration at $\theta = \pi$ would be crucial to precisely check if the ALP domain wall annihilation can still be viable to account for the NANOGrav 15-year data. The related spike structure, following the order of the phase transition, the first order or the second order, would be subject to effective model approaches for QCD [16,35–47,49–51]. The presently employed NJL-type model with the MFA tends to predict the second order [40,42,43], while the linear-sigma model type with the MFA [16,37–42] and the 't Hooft anomaly matching argument [50,51] supports the first order phase transition. Even going beyond the MFA and/or the RPA, including subleading order contributions in $1/N_c$ expansion, the presently claimed incompatibility would be crucial to deduce a more definite conclusion of the compatibility of the ALP domain wall interpretation with NANOGrav 15-year data. The functional renormalization group analysis makes it possible to clarify the case, which deserves to another publication. At any rate, the presently claimed incompatibility would still pin down one benchmark point in the full parameter space of the QCD-biased ALP domain wall collapse.

(v) As seen from Figs. 3 and 4 in Appendix B, at $\theta = \pi$ the thermal *CP* restoration point coincides with the pseudocritical point (inflection point) for the chiral crossover. This is due to the present MFA, which involves the two intrinsic features at $\theta = \pi$: (i) the
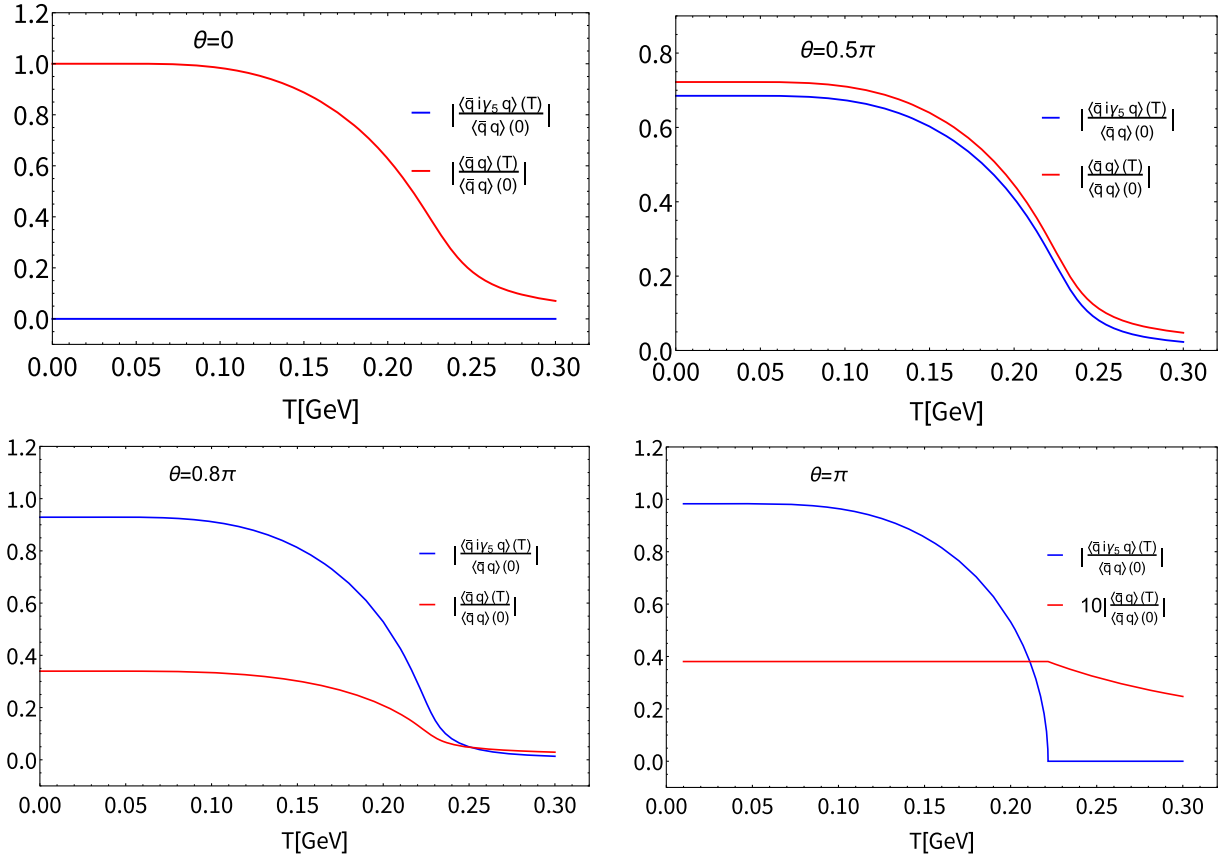
FIG. 3.   Scalar and pseudoscalar condensates normalized to the scalar condensate at $T = \theta = 0$ versus temperature at nonzero θ.

chiral symmetry is not spontaneously broken via the scalar quark condensate $\langle \bar{q}q \rangle$, as long as the *CP* symmetry is broken; (ii) no $U(1)$ axial violating loop corrections are generated at this approximation level. Those lead to no thermal development of $\langle \bar{q}q \rangle$ until the *CP* symmetry restores, hence $\langle \bar{q}q \rangle$ gets kicked down instantaneously, i.e., undergoes the pseudocritical point at the same timing as the *CP* restoration. We have clarified those points in Appendix B [around Eq. (B15)]. Going beyond the MFA analysis, such as the functional renormalization group, would potentially generate a gap between two critical points for the (effective) chiral and *CP* symmetry restorations, which should come from the $U(1)$ axial anomaly effects in loops. The further investigation along this line could also make a complementary benchmark compared to the prediction from the 't Hooft-anomaly matching in pure Yang-Mills theories [67], which suggests the *CP* restoration temperature is higher than or equal to the deconfinement phase transition one.

(vi) When strange quark contributions are incorporated in the analysis, the thermal *CP* restoration at $\theta = \pi$ would be more involved. First of all, one notices that the *CP* phase contribution carried by the strange quark is highly suppressed by a factor of $m_{u,d}/m_s$, as

reviewed in Appendix A [around Eqs. (A10)–(A12)]. This observation comes from the robust flavor singlet nature of the θ dependence in QCD that requires the strange quark field to carry the θ phase with the form $e^{i\frac{m_{u,d}}{2m_s}\theta} \simeq 1$, i.e., almost free from θ. Thus, as far as the *CP* violating effects are concerned, the three-flavor QCD is essentially decomposed into the $2 + 1$ (the lightest two quarks and the strange quark) structure and the *CP* order parameter is almost controlled by the lightest two-flavor sector, i.e., $\sum_{q=u,d} \langle \bar{q}i\gamma_5 q \rangle$.

This is the characteristic flavor violation and irrespective to the presence of the QCD topological charge fluctuation, which is flavor universal, or equivalently in the NJL framework, the 't Hooft-Kobayashi-Maskawa determinant term [68–71] (as in Appendix B). In the three-flavor NJL with the MFA, thus the chiral crossover for $\langle \bar{s}s \rangle$ would still persist even at $\theta = \pi$, simply because of presence of the finite strange quark mass, while $\langle \bar{q}q \rangle$ would be subject to the approximation for QCD, or the (P) NJL. In the MFA of the three-flavor NJL, $\langle \bar{q}q \rangle$ would be trapped to a constant value until the *CP* phase transition takes place at $T = T_c$, and then starts to drops when $T > T_c$ (with discontinuity in the T-derivative at $T = T_c$), as in the two-flavor case
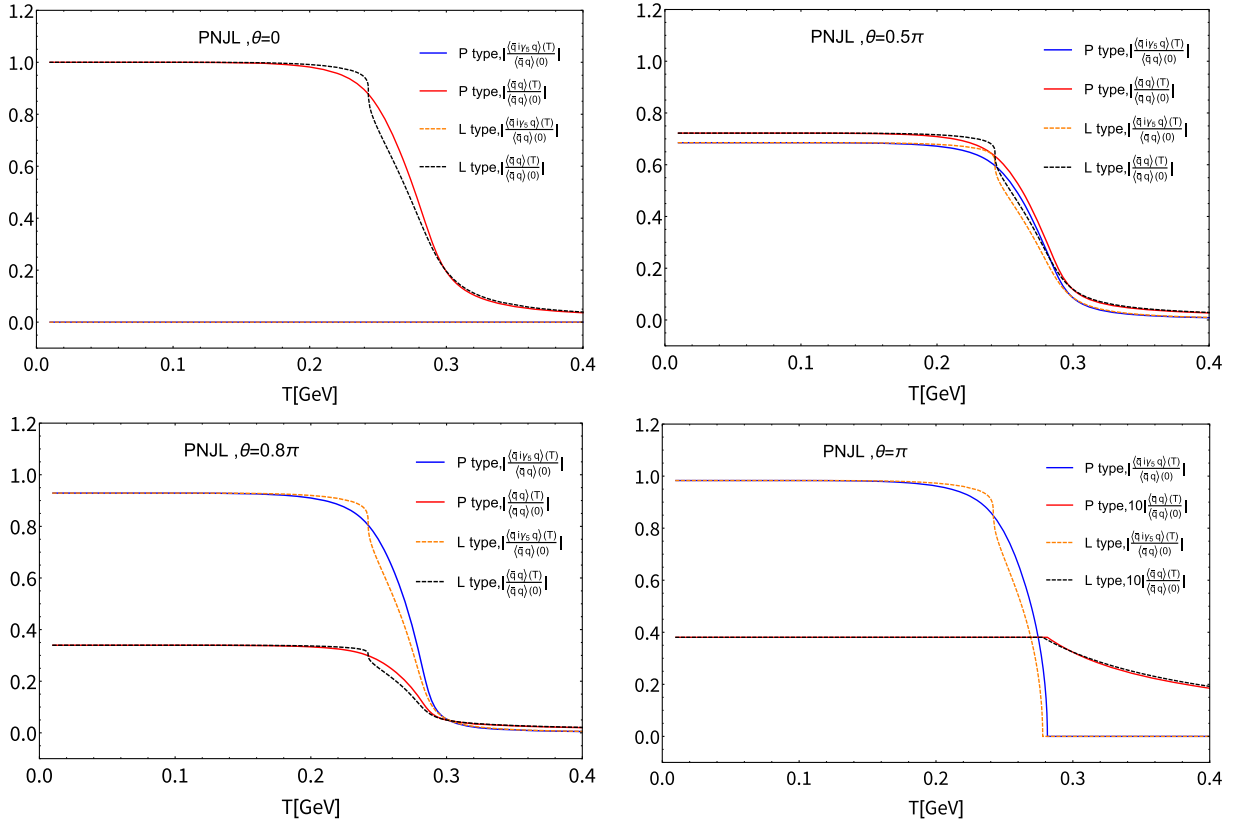
FIG. 4. Scalar and pseudoscalar condensates normalized to the scalar condensate at $T = 0$ and $\theta = 0$ versus temperature with varying θ from 0. The abbreviations L and P denote the PL potential of logarithmic and polynomial type, respectively.

(Fig. 3 in Appendix B). As in the case with $\theta = 0$, $\langle \bar{s}s \rangle$ would drop down with T more slowly than $\langle \bar{q}q \rangle$ simply due to the larger strange quark mass. Thus, in the framework of the MFA of the NJL, the *CP* phase transition in the three-flavor case would be essentially identical to the one in the lightest two-flavor case, hence it would still be of the second order keeping the critical spike structure of χ_{top}, hence α_* does as well, as seen from Fig. 2.

However, as has been discussed in the recent literature [72–74] based on the functional renormalization group analysis on the three-flavor linear sigma model with $\theta = 0$, the 't Hooft-Kobayashi-Maskawa determinant term beyond the MFA could be nonperturbatively enhanced at around $T = T_c$ even in the case of $\theta = \pi$. This implies that the criticality of the *CP* phase transition as well as the chiral phase transition might significantly be altered and the entry of the strange quark contributions beyond the MFA might be nontrivial, though the carried *CP* phase is intrinsically highly suppressed as aforementioned. Thus, the detailed analysis in the three-flavor NJL, both within and beyond the MFA, is noteworthy to pursue in another publication.

Finally, we comment on impacts of lattice QCD calculations to this observation. Most of current lattice QCD calculations at the physical point have been done using the Monte-Carlo method. For nonzero theta, simulations are suffered from infamous sign problem. Namely, we cannot calculate expectation values with $|\theta| \gg 0$. To avoid the problem in the realistic setup, we employ imaginary theta and analytic continue to the real theta to get expectation values for physical observables [75–82]. These calculations for χ_{top} have been done away from the physical point. An interesting methods for nonzero theta is suggested [83], but it is still hard to get physical results. Digital and analog quantum simulations and calculations with nonzero theta using tensor networks have been performed for toy models but not for the realistic setup like four dimensional QCD at the physical point [84–89].

APPENDIX A: GENERIC PROPERTIES OF ANOMALOUS CHRIAL WARD-TAKAHASHI IDENTITIES (ACWTIS) IN QCD

1. ACWTIs with external gauge fields and θ

We start with the QCD Lagrangian with N_f quarks including the external gauge fields,

$$\mathcal{L}_{\text{QCD}} = \bar{q}_L i\gamma^\mu D_\mu q_L + \bar{q}_R i\gamma^\mu D_\mu q_R - \bar{q}_L \mathbf{m}_f q_R - \bar{q}_R \mathbf{m}_f q_L$$
$$+ \frac{1}{2} \sum_{a=1}^{8} \text{tr}[(G_{\mu\nu}^a T_c^a)^2] + \theta \frac{g^2}{64\pi^2} \epsilon^{\mu\nu\rho\sigma} G_{\mu\nu}^a G_{\rho\sigma}^a, \quad \text{(A1)}$$

where $q_{L(R)}$ denotes the left-(right-) handed quark fields belong to the fundamental representation of $SU(N_f)$; $\mathbf{m}_f$ is the current quark mass for f-quark taking the diagonal form

like $\mathbf{m}_f = \text{diag}(m_u, m_d, \cdots)$; $G_{\mu\nu}^a$ ($a = 0, 1, \ldots, 8$) are the field strengths of the gluon fields G_μ^a; T_c^a stand for the generators of the QCD color group $SU(3)_c$; g denotes the QCD gauge coupling constant; $\theta = \theta(x)$ plays the role of the source for the topological operator $ig^2\epsilon^{\mu\nu\rho\sigma}G_{\mu\nu}^a G_{\rho\sigma}^a$; The external gauge fields $\mathcal{L}_\mu^A$ and $\mathcal{R}_\mu^A$ ($A = 0, \ldots, N_f^2 - 1$) are introduced by gauging the global chiral $U(N_f)_L$ and $U(N_f)_R$ symmetry, which are embedded into the covariant derivatives as

$$D_\mu q_L = (\partial_\mu - igG_\mu^a T_c^a - i\mathcal{L}_\mu^A T_f^A)q_L,$$
$$D_\mu q_R = (\partial_\mu - igG_\mu^a T_c^a - i\mathcal{R}_\mu^A T_f^A)q_R, \quad \text{(A2)}$$

with T_f^A being the generators of $U(N_f)$ in the flavor space.

The vacuum energy of QCD is given by

$$V_{\text{QCD}}(\theta) = -i \ln Z_{\text{QCD}}, \quad \text{(A3)}$$

where Z_{QCD} represents the generating functional of QCD in Minkowski spacetime,

$$Z_{\text{QCD}} = \int [dqd\bar{q}][dG] \exp\left[i \int d^4x \mathcal{L}_{\text{QCD}}\right]. \quad \text{(A4)}$$

We define the topological susceptibility χ_{top} including the θ dependence:

$$\chi_{\text{top}}(\theta) = -\int d^4x \frac{\delta^2 V_{\text{QCD}}(\theta)}{\delta\theta(x)\delta\theta(0)} - i \int d^4x \frac{\delta V_{\text{QCD}}}{\delta\theta(x)} \frac{\delta V_{\text{QCD}}}{\delta\theta(0)}$$
$$= -i \int d^4x \langle 0|T\left(\frac{g^2}{64\pi^2}\epsilon^{\mu\nu\rho\sigma}G_{\mu\nu}^a G_{\rho\sigma}^a\right)(x)\left(\frac{g^2}{64\pi^2}\epsilon^{\mu\nu\rho\sigma}G_{\mu\nu}^b G_{\rho\sigma}^b\right)(0)|0\rangle_\theta, \quad \text{(A5)}$$

where we have introduced the subscript θ to explicitize the θ dependence on the vacuum.

The external fields, such as the electromagnetic field A_μ, the baryon chemical potential μ_B, and the chiral chemical potential μ_5, are embedded in the external gauge fields as[5]

$$\mathcal{L}_\mu^A T_f^A = \left[eQ_{\text{em}}A_\mu + \frac{\mu_B}{3}\mathbf{1}_{N_f\times N_f}\right] - [\mu_5\mathbf{1}_{N_f\times N_f}],$$
$$\mathcal{R}_\mu^a T_f^a = \left[eQ_{\text{em}}A_\mu + \frac{\mu_B}{3}\mathbf{1}_{N_f\times N_f}\right] + [\mu_5\mathbf{1}_{N_f\times N_f}], \quad \text{(A6)}$$

where e represents the electromagnetic coupling constant, and Q_{em} denotes the electric charge matrix for quarks $Q_{\text{em}} = \text{diag}(Q_{\text{em}}^u, Q_{\text{em}}^d, \cdots)$. The chemical potentials have

been introduced as constant fields. In QCD with the external gauge fields, the $U(1)_A$ symmetry is explicitly broken by the current quark mass term and the gluonic quantum anomaly, and also external electromagnetic field. This is reflected in the anomalous conservation law of the $U(1)$ axial current for each quark in the N_f-plet quark field q, labeled as q_f,

$$\partial_\mu j_A^{(f)\mu} = 2i\bar{q}^f m_f \gamma_5 q^f + \frac{g^2}{32\pi^2}\epsilon^{\mu\nu\rho\sigma}G_{\mu\nu}^a G_{\rho\sigma}^a$$
$$+ N_c \frac{e^2[Q_{\text{em}}^f]^2}{32\pi^2}\epsilon^{\mu\nu\rho\sigma}F_{\mu\nu}F_{\rho\sigma}, \quad \text{(A7)}$$

with the $U(1)$ axial current $j_A^{(f)\mu} = \bar{q}^f\gamma_5\gamma^\mu q^f$. Note that the constant chemical potentials do not contribute to the anomalous conservation law.

Under the $U(1)_A$ rotation with the rotation angle α_A, the quark fields transform as

---

[5]The isospin chemical potential can also be incorporated, when $N_f = 2$, into the covariant derivative as an additional external gauge field term proportional to ($\sigma^3/2$).

$$q_L^f \rightarrow \exp(-i\alpha_A^f/2)q_L^{\prime f},$$
$$q_R^f \rightarrow \exp(+i\alpha_A^f/2)q_R^{\prime f}. \tag{A8}$$

Then the QCD generating functional gets shifted as

$$\int [dq' d\bar{q}'][dG] \exp\left[i \int d^4x \left(\bar{q}_L' i\gamma^\mu D_\mu q_L' + \bar{q}_R' i\gamma^\mu D_\mu q_R' - \sum_f (\bar{q}_L^{\prime f} m_f e^{i\alpha_A^f} q_R^{\prime f} + \bar{q}_R^{\prime f} m_f e^{-i\alpha_A^f} q_L^{\prime f}) + \frac{1}{2}\sum_{a=1}^8 \text{tr}[(G_{\mu\nu}^a T_c^a)^2] \right. \right.$$

$$\left. \left. + \left(\theta - \sum_f \alpha_A^f\right) \frac{g^2}{64\pi^2} \epsilon^{\mu\nu\rho\sigma} G_{\mu\nu}^a G_{\rho\sigma}^a - \left(\sum_f \alpha_A^f Q_f^2\right) N_c \frac{e^2}{64\pi^2} \epsilon^{\mu\nu\rho\sigma} F_{\mu\nu} F_{\rho\sigma} \right) \right]. \tag{A9}$$

To rotate the QCD θ term away, we take the following phase choice reflecting the flavor-singlet nature of the QCD vacuum [30–32,34],

$$\alpha_A^f = \frac{\bar{m}}{m_f}\theta, \tag{A10}$$

with

$$\bar{m} = \left(\sum_f \frac{1}{m_f}\right)^{-1}. \tag{A11}$$

Then the QCD generating functional goes like

$$Z_{\text{QCD}} = \int [dq' d\bar{q}'][dG] \exp\left[i \int d^4x \left(\bar{q}_L' i\gamma^\mu D_\mu q_L' + \bar{q}_R' i\gamma^\mu D_\mu q_R' + \frac{1}{2}\sum_{a=1}^8 \text{tr}[(G_{\mu\nu}^a T_c^a)^2] \right. \right.$$

$$\left. \left. - \sum_f \left(\bar{q}_L^{\prime f} m_f \exp\left(i\frac{\bar{m}}{m_f}\theta\right) q_R^{\prime f} + \bar{q}_R^{\prime f} m_f \exp\left(-i\frac{\bar{m}}{m_f}\theta\right) q_L^{\prime f} \right) - \left(\sum_f \frac{\bar{m}}{m_f}\theta Q_f^2\right) N_c \frac{e^2}{64\pi^2} \epsilon^{\mu\nu\rho\sigma} F_{\mu\nu} F_{\rho\sigma} \right) \right]. \tag{A12}$$

From this generating functional, the topological susceptibility is given as

$$\chi_{\text{top}}(\theta) = \chi_{\text{top}}^{(0)}(\theta) + \chi_{\text{top}}^{(\text{EM})}(\theta), \tag{A13}$$

where

$$\chi_{\text{top}}^{(0)}(\theta) = -\bar{m}^2 \left[\sum_f \frac{1}{m_f} \langle 0|\left(\bar{q}^{\prime f} q^{\prime f} \cos\frac{\theta}{2} + \bar{q}^{\prime f} i\gamma_5 q^{\prime f} \sin\frac{\theta}{2} \right)|0\rangle_\theta \right.$$

$$\left. + i \int d^4x \langle 0|T \sum_f \left(\bar{q}^{\prime f} i\gamma_5 q^{\prime f} \cos\frac{\theta}{2} - \bar{q}^{\prime f} q^{\prime f} \sin\frac{\theta}{2} \right)(x) \sum_{f'} \left(\bar{q}^{\prime f'} i\gamma_5 q^{\prime f'} \cos\frac{\theta}{2} - \bar{q}^{\prime f'} q^{\prime f'} \sin\frac{\theta}{2} \right)(0)|0\rangle_\theta \right],$$

$$\chi_{\text{top}}^{(\text{EM})}(\theta) = -i\left(\sum_f \frac{\bar{m} Q_f^2}{m_f}\right)^2 \int d^4x \langle 0|T \left(\frac{e^2 N_c}{64\pi^2} \epsilon^{\mu\nu\rho\sigma} F_{\mu\nu} F_{\rho\sigma} \right)(x) \left(\frac{e^2 N_c}{64\pi^2} \epsilon^{\mu\nu\rho\sigma} F_{\mu\nu} F_{\rho\sigma} \right)(0)|0\rangle_\theta$$

$$- i\left(\sum_f \frac{\bar{m}^2 Q_f^2}{m_f}\right) \int d^4x \langle 0|T \left(\frac{e^2 N_c}{64\pi^2} \epsilon^{\mu\nu\rho\sigma} F_{\mu\nu} F_{\rho\sigma} \right)(x) \sum_f \left(\bar{q}^{\prime f} i\gamma_5 q^{\prime f} \cos\frac{\theta}{2} - \bar{q}^{\prime f} q^{\prime f} \sin\frac{\theta}{2} \right)(0)|0\rangle_\theta$$

$$- i\left(\sum_f \frac{\bar{m}^2 Q_f^2}{m_f}\right) \int d^4x \langle 0|T \left(\bar{q}^{\prime f} i\gamma_5 q^{\prime f} \cos\frac{\theta}{2} - \bar{q}^{\prime f} q^{\prime f} \sin\frac{\theta}{2} \right)(x) \left(\frac{e^2 N_c}{64\pi^2} \epsilon^{\mu\nu\rho\sigma} F_{\mu\nu} F_{\rho\sigma} \right)(0)|0\rangle_\theta. \tag{A14}$$

These susceptibilities are written in terms of the primed quark field q'. They can be rewritten in terms of the original quark field q using the following connection,

$$q = \exp(i\theta\gamma_5/4)q'. \tag{A15}$$

Then $\chi_{\text{top}}^{(0)}(\theta)$ and $\chi_{\text{top}}^{(\text{EM})}(\theta)$ go like

$$\chi_{\text{top}}^{(0)}(\theta) = -\bar{m}^2\left[\sum_f \frac{1}{m_f}\langle 0|\bar{q}^f q^f|0\rangle + i\int d^4x \langle 0|T\left(\sum_f \bar{q}^f i\gamma_5 q^f\right)(x)\left(\sum_{f'} \bar{q}^{f'} i\gamma_5 q^{f'}\right)(0)|0\rangle\right]_\theta,$$

$$\chi_{\text{top}}^{(\text{EM})}(\theta) = -i\left(\sum_f \frac{\bar{m}Q_f^2}{m_f}\right)^2 \int d^4x \langle 0|T\left(\frac{e^2 N_c}{64\pi^2}\epsilon^{\mu\nu\rho\sigma}F_{\mu\nu}F_{\rho\sigma}\right)(x)\left(\frac{e^2 N_c}{64\pi^2}\epsilon^{\mu\nu\rho\sigma}F_{\mu\nu}F_{\rho\sigma}\right)(0)|0\rangle_\theta$$

$$- i\left(\sum_f \frac{\bar{m}^2 Q_f^2}{m_f}\right)\int d^4x \langle 0|T\left(\frac{e^2 N_c}{64\pi^2}\epsilon^{\mu\nu\rho\sigma}F_{\mu\nu}F_{\rho\sigma}\right)(x)\left(\sum_f \bar{q}^f i\gamma_5 q^f\right)(0)|0\rangle_\theta$$

$$- i\left(\sum_f \frac{\bar{m}^2 Q_f^2}{m_f}\right)\int d^4x \langle 0|T\left(\sum_f \bar{q}^f i\gamma_5 q^f\right)(x)\left(\frac{e^2 N_c}{64\pi^2}\epsilon^{\mu\nu\rho\sigma}F_{\mu\nu}F_{\rho\sigma}\right)(0)|0\rangle_\theta. \tag{A16}$$

The χ_{top} term in Eq. (A13) is precisely the generalization of the one in Eq. (4) with Eq. (5), which has also been addressed in the literature [30–32,34] without external gauge fields. Thus the presence of the electromagnetic axial anomaly yields additional topological susceptibility, $\chi_{\text{top}}^{(\text{EM})}$.

Next, we evaluate the ACWTIs for $SU(N_f)_L \times SU(N_f)_R$ transformation in QCD. Under the chiral $SU(N_f)$ transformation, the quark field q transforms as

$$q(x) \to q(x) + i\alpha^A(x)T^A\gamma_5 q(x), \qquad A = 1, \cdots N_f^2 - 1. \tag{A17}$$

Then, the chiral $SU(N_f)$ transformation of the expectation value for an arbitrary local operator $\mathcal{O}(x_1)$ in the path integral formalism yields the ACWTIs:

$$\int d^4x \lim_{\alpha^A \to 0}\left\langle \frac{\delta\mathcal{O}'(x_1)}{\delta\alpha^A(x)}\right\rangle_\theta + \int d^4x\langle \mathcal{O}(x_1)iD_\mu j_5^{A\mu}(x)\rangle_\theta$$

$$+ \int d^4x\langle \mathcal{O}(x_1)\bar{q}\{\mathbf{m}_f, T^A\}\gamma_5 q(x)\rangle_\theta = 0, \tag{A18}$$

where $j_5^{A\mu}$ denotes the chiral $SU(N_f)$ current, $j_5^{A\mu} = \bar{q}\gamma^\mu\gamma_5 T^A q$, and

$$D_\mu j_5^{A\mu} = \partial_\mu j_5^{A\mu} - i[\mathcal{V}_\mu, j_5^{A\mu}], \tag{A19}$$

with $\mathcal{V}_\mu = (\mathcal{R}_\mu + \mathcal{L}_\mu)/2$. Equation (A18) is a generalization of the ACWTIs addressed in [30–32,34] without external gauge fields. Unless external gauge fields possess a topologically nontrivial configuration, we can rewrite the covariant derivative term as

$$\int d^4x\langle \mathcal{O}(x_1)iD_\mu j_5^{A\mu}(x)\rangle_\theta$$

$$= i\int d^4x D_\mu^{(x)}\langle 0|T\mathcal{O}(x_1)j_5^{A\mu}(x)|0\rangle_\theta$$

$$= \text{surface term}. \tag{A20}$$

Thus we eventually have

$$\int d^4x \lim_{\alpha^A \to 0}\left\langle \frac{\delta\mathcal{O}'(x_1)}{\delta\alpha^A(x)}\right\rangle_\theta$$

$$+ \int d^4x\langle \mathcal{O}(x_1)\bar{q}\{\mathbf{m}_f, T^A\}\gamma_5 q(x)\rangle_\theta = 0. \tag{A21}$$

This implies that the ACWTIs keep the same form as those in the case without external gauge fields [30–32,34].

For instance, in the case of $N_f = 3$, we find the same form of the ACWTIs as in the literature [30–32,90]:

$$\langle \bar{u}u\rangle_\theta + \langle \bar{d}d\rangle_\theta = -m_l\chi_\pi(\theta),$$

$$\langle \bar{u}u\rangle_\theta + \langle \bar{d}d\rangle_\theta + 4\langle \bar{s}s\rangle_\theta = -[m_l(\chi_P^{uu} + \chi_P^{dd} + 2\chi_P^{ud}) - 2(m_s + m_l)(\chi_P^{us} + \chi_P^{ds}) + 4m_s\chi_P^{ss}]_\theta,$$

$$\langle \bar{u}u\rangle_\theta + \langle \bar{d}d\rangle_\theta - 2\langle \bar{s}s\rangle_\theta = -[m_l(\chi_P^{uu} + \chi_P^{dd} + 2\chi_P^{ud}) + (m_l - 2m_s)(\chi_P^{us} + \chi_P^{ds}) - 2m_s\chi_P^{ss}]_\theta, \tag{A22}$$

with $m_l = m_u = m_d$. Here $\chi_\pi(\theta)$ denotes the pion susceptibility defined as

$$\chi_\pi(\theta) = \int_T d^4x[\langle(\bar{u}(0)i\gamma_5 u(0))(\bar{u}(x)i\gamma_5 u(x))\rangle_{\text{conn}} + \langle(\bar{d}(0)i\gamma_5 d(0))(\bar{d}(x)i\gamma_5 d(x))\rangle_{\text{conn}}]_\theta, \tag{A23}$$

with $\langle\cdots\rangle_{\text{conn}}$ being the connected part of the correlation function, and the pseudoscalar susceptibilities $\chi_P^{uu,dd,ud}$, χ_P^{ss} and $\chi_P^{us,ds}$ are defined as

$$\chi_P^{f_1 f_2}(\theta) = \int_T d^4x\langle(\bar{q}_{f_1}(0)i\gamma_5 q_{f_1}(0))(\bar{q}_{f_2}(x)i\gamma_5 q_{f_2}(x))\rangle_\theta, \quad \text{for } q_{f_{1,2}} = u, d, s. \tag{A24}$$

$\chi_{\text{top}}^{(0)}(\theta)$ in Eq. (A16) then takes a couple of equivalent forms, related each other by the ACWTIs in Eq. (A22) [30–32,34]

$$
\begin{aligned}
\chi_{\text{top}}^{(0)}(\theta) &= \bar{m}^2\left[\frac{\langle\bar{u}u\rangle}{m_l} + \frac{\langle\bar{d}d\rangle}{m_l} + \frac{\langle\bar{s}s\rangle}{m_s} + \chi_P^{uu} + \chi_P^{dd} + \chi_P^{ss} + 2\chi_P^{ud} + 2\chi_P^{us} + 2\chi_P^{ds}\right]_\theta \\
&= \frac{1}{4}[m_l(\langle\bar{u}u\rangle + \langle\bar{d}d\rangle) + m_l^2(\chi_P^{uu} + \chi_P^{dd} + 2\chi_P^{ud})]_\theta \\
&= \frac{m_l^2}{4}(\chi_\pi(\theta) - \chi_\eta(\theta)) \\
&= m_s\langle\bar{s}s\rangle_\theta + m_s^2\chi_P^{ss}(\theta),
\end{aligned}
\tag{A25}
$$

with $\bar{m} = (\frac{2}{m_l} + \frac{1}{m_s})^{-1}$. It is interesting to note that χ_π and χ_η are related not to the full topological susceptibility χ_{top}, but $\chi_{\text{top}}^{(0)}$, in Eq. (A13).

2. Renormalization group invariance of χ_{top}

The current quark mass parameter is multiplicatively renormalized as

$$m_f^0(\Lambda) = Z_S^{-1}(\Lambda, \mu)m_f^R(\mu), \tag{A26}$$

where Λ denotes the bare cutoff and the upper script R stands for the quantity renormalized at the scale μ. When the mass independent renormalization is thus applied. the renormalization factor Z_S^{-1} is flavor universal. Then we are allowed to drop the flavor label f as

$$\bar{m}^0(\Lambda) = Z_S^{-1}(\Lambda, \mu)\bar{m}^R(\mu). \tag{A27}$$

This also implies that Z_S is independent of the current quark mass as well.

The $\bar{q}_f q_f$ bilinear operator is also multiplicatively renormalized by $Z_S(\lambda, \mu)$,

$$(\bar{q}_f q_f)_R = Z_S^{-1}(\Lambda, \mu)(\bar{q}_f q_f)_\Lambda, \tag{A28}$$

so that we have the renormalization group invariant mass term like

$$m_f^0(\Lambda)(\bar{q}_f q_f)_\Lambda = m_f^R(\mu)(\bar{q}_f q_f)_R. \tag{A29}$$

Consider also a $(\bar{q}_f i\gamma_5 q_f)$ operator to be renormalized in a similar way with the renormalization constant $Z_P^{-1}(\lambda, \mu)$

$$(\bar{q}_f i\gamma_5 q_f)_R = Z_P^{-1}(\Lambda, \mu)(\bar{q}_f i\gamma_5 q_f)_\Lambda. \tag{A30}$$

Since none of quark mass dependence is generated in the mass independent renormalization, the $U(1)$ axial invariance keeps manifest between renormalization of the $(\bar{q}_f q_f)$ and $(\bar{q}_f i\gamma_5 q_f)$ operators. Hence we have

$$Z_P^{-1} = Z_S^{-1}. \tag{A31}$$

In that case we also find

$$(\chi_P^{f_1 f_2})_\Lambda = Z_S^2(\chi_P^{f_1 f_2})_R, \tag{A32}$$

Now, we apply the renormalization procedure as above to $\chi_{\text{top}}^{(0)}$ in the three-flavor case [Eq. (A25)]:

$$
\begin{aligned}
(\chi_{\text{top}}^{(0)})_\Lambda &= -\bar{m}_0^2\left[\frac{\langle(\bar{u}u)_\Lambda\rangle}{m_u^0} + \frac{\langle(\bar{d}d)_\Lambda\rangle}{m_d^0} + \frac{\langle(\bar{s}s)_\Lambda\rangle}{m_s^0} + i(\chi_P^{uu})_\Lambda + i(\chi_P^{dd})_\Lambda + i(\chi_P^{ss})_\Lambda + 2i(\chi_P^{ud})_\Lambda + 2i(\chi_P^{us})_\Lambda + 2i(\chi_P^{ds})_\Lambda\right] \\
&= -\bar{m}_R^2\left[\frac{\langle(\bar{u}u)_R\rangle}{m_u^R} + \frac{\langle(\bar{d}d)_R\rangle}{m_d^R} + \frac{\langle(\bar{s}s)_R\rangle}{m_s^R} + i(\chi_P^{uu})_R + i(\chi_P^{dd})_R + i(\chi_P^{ss})_R + 2i(\chi_P^{ud})_R + 2i(\chi_P^{us})_R + 2i(\chi_P^{ds})_R\right] \\
&= (\chi_{\text{top}}^{(0)})_R.
\end{aligned}
\tag{A33}
$$

Thus it has been proven that $\chi_{\text{top}}^{(0)}$ is renormalization group invariant. Note that this argument is also applicable to the case with nonzero θ, because the QCD θ is itself conventionally renormalization group invariant and no new divergent terms induced due to nonzero θ will be generated, hence the renormalization factors will not be corrected. Furthermore, one can readily see that the external gauge-induced $\chi_{\text{top}}^{\text{EM}}$, defined as in Eq. (A14), is also manifestly renormalization group invariant.

APPENDIX B: THE DETAILS ON THE (P)NJL MODEL ANALYSIS

1. NJL case

Our reference NJL Lagrangian with two flavors (up and down quarks) and nonzero θ follows the literature [43], which takes the form

$$\mathcal{L} = \bar{q}(i\gamma_\mu\partial^\mu - m)q + \frac{g_s}{2}\sum_{a=0}^{3}[(\bar{q}\tau_a q)^2 + (\bar{q}i\gamma_5\tau_a q)^2]$$
$$+ g_d(e^{i\theta}\det[\bar{q}(1+\gamma_5)q] + e^{-i\theta}\det[\bar{q}(1-\gamma_5)q]),$$
$$(B1)$$

where $q = (u, d)^T$ and the determinant acts on the quark flavors. The g_d term, called the 't Hooft-Kobayashi-Maskawa determinant term [68–71], breaks $U(1)$ axial symmetry, but keeps $SU(2)_L \times SU(2)_R \times U(1)_V$ symmetry, while others keep the full chiral $U(2)_L \times U(2)_R$ symmetry. The g_d term thus serves as the $U(1)$ axial anomaly:

$$\partial_\mu j_A^\mu = 2i\bar{q}m\gamma_5 q - 8g_d\text{Im}[\det\bar{q}(1-\gamma_5)q \cdot e^{-i\theta}]. \quad (B2)$$

Since the $U(1)$ axial symmetry is broken only by g_d and the quark mass terms, one can move θ in the g_d term to the mass term by a $U(1)$ axial rotation as was done in the case of the general argument above:

$$q \to e^{-i\gamma_5\frac{\theta}{2}}q \equiv q', \quad (B3)$$

so that

$$\mathcal{L} \to \mathcal{L}' = \bar{q}'(i\gamma_\mu\partial^\mu - m(\theta))q'$$
$$+ \frac{g_s}{2}\sum_{a=0}^{3}[(\bar{q}'\tau_a q')^2 + (\bar{q}'i\gamma_5\tau_a q')^2]$$
$$+ g_d(\det[\bar{q}'(1+\gamma_5)q'] + \text{H.c.}), \quad (B4)$$

where

$$m(\theta) = m\left[\cos\frac{\theta}{2} + i\gamma_5\sin\frac{\theta}{2}\right], \quad (B5)$$

in which nonzero θ manifestly signals the *CP* violation. Use of this "prime" basis is convenient to analyze the model because all the θ dependence is transformed and collected into the complex mass $m(\theta)$ in the quark propagator. Similarly to Eqs. (1) and (B3) relates the scalar and pseudoscalar bilinears between the original- and prime-base scalar and pseudoscalar bilinears (for each quark flavor i) as

$$(\bar{q}_i q_i) = (\bar{q}'_i q'_i)\cos\frac{\theta}{2} + (\bar{q}'_i i\gamma_5 q'_i)\sin\frac{\theta}{2},$$
$$(\bar{q}_i i\gamma_5 q_i) = -(\bar{q}'_i q'_i)\sin\frac{\theta}{2} + (\bar{q}'_i i\gamma_5 q'_i)\cos\frac{\theta}{2}. \quad (B6)$$

We work in the MFA, so that the scalar and pseudoscalar bilinears $(\bar{q}'_i q'_i)$ and $(\bar{q}'_i i\gamma_5 q'_i)$ are expanded around the means fields $S' = \langle\bar{q}'_i q'_i\rangle$ and $P' = \langle\bar{q}'_i i\gamma_5 q'_i\rangle$, as $\bar{q}'_i q'_i = S' + (:\bar{q}'_i q'_i:)$ and $\bar{q}'_i i\gamma_5 q'_i = P' + (:\bar{q}'_i i\gamma_5 q'_i:)$, where the terms sandwiched by ":" stand for the normal ordered product, meaning that $\langle:\mathcal{O}:\rangle = 0$ for $\mathcal{O} = S', P'$. Then the interaction terms in Eq. (B1) are replaced, up to the normal ordered terms, as

$$(\bar{q}'_i q'_i)^2 \to 4S'\sum_i(\bar{q}'_i q'_i) - 4S'^2,$$

$$(\bar{q}'_i i\gamma_5 q'_i)^2 \to 4P'\sum_i(\bar{q}'_i i\gamma_5 q'_i) - 4P'^2,$$

$$\det[\bar{q}'_i(1+\gamma_5)q'_i] + \text{H.c.} \to 2S'\sum_i(\bar{q}'_i q'_i) - 2P'\sum_i(\bar{q}'_i i\gamma_5 q'_i) - 2(S'^2 - P'^2). \quad (B7)$$

In the MFA the NJL Lagrangian in Eq. (B1) thus takes the form

$$\mathcal{L}_{\text{MFA}} = \sum_i \bar{q}'_i(i\gamma_\mu\partial^\mu - \mathcal{M}(S', P'; \theta))q'_i - 2g_s(S'^2 + P'^2) - 2g_d(S'^2 - P'^2), \quad (B8)$$

with

$$\mathcal{M}(S', P'; \theta) = \alpha(S'; \theta) + i\gamma_5 \beta(P'; \theta),$$

$$\alpha(S'; \theta) = m\cos\frac{\theta}{2} - 2(g_s + g_d)S',$$

$$\beta(P'; \theta) = m\sin\frac{\theta}{2} - 2(g_s - g_d)P'. \qquad (B9)$$

Integrating out quarks leads to the thermodynamic potential in the MFA:

$$\Omega[S', P'; \theta] = 2g_s(S'^2 + P'^2) + 2g_d(S'^2 - P'^2)$$
$$- 2N_cN_f \int \frac{d^3k}{(2\pi)^3} [E + 2T\ln(1 + e^{-E/T})], \qquad (B10)$$

where $N_f = 2$ and $N_c = 3$, and

$$E = \sqrt{M^2 + k^2}, \qquad M^2 = \alpha^2 + \beta^2, \qquad (B11)$$

with $k^2 = |\vec{k}|^2$. Then $\langle \bar{q}_i' q_i' \rangle = S'$ and $\langle \bar{q}_i' i\gamma_5 q_i' \rangle = P'$ are determined through the stationary condition,

$$\frac{\partial \Omega}{\partial S'} = \frac{\partial \Omega}{\partial P'} = 0. \qquad (B12)$$

Of particular interest is to see the thermodynamic potential at $\theta = \pi$,

$$\Omega[\alpha, \beta; \theta = \pi] = \frac{1}{2g_s + 2g_D}\alpha^2 + \frac{1}{2g_s - 2g_D}(\beta - m)^2$$
$$- 2N_cN_f \int \frac{d^3p}{(2\pi)^3} [E + 2T\ln(1 + e^{-E/T})], \qquad (B13)$$

where things have been written in terms of α and β by means of Eq. (B9). In the presently applied MFA, the loop corrections [corresponding to the last term in Eq. (B13)] are $U(1)$ axial invariant, i.e., do not separate α and β due to no loop contributions involving vertices with the determinant coupling g_d. At $\theta = \pi$, the explicit-chiral $SU(2)$ breaking-effect (by m) has completely been transported into the β direction (the second term). The stationary condition then takes the form

$$\alpha = 2N_cN_f(g_s + g_D)\alpha \int \frac{d^3p}{(2\pi)^3} \frac{1}{E}\left[1 - \frac{2}{1 + e^{E/T}}\right],$$

$$\beta - m = 2N_cN_f(g_s - g_D)\beta \int \frac{d^3p}{(2\pi)^3} \frac{1}{E}\left[1 - \frac{2}{1 + e^{E/T}}\right]. \qquad (B14)$$

When $\alpha \neq 0$, i.e., the *CP* symmetry is spontaneously broken, the gap equation for β can be rewritten by

eliminating the loop correction part as

$$\beta - m = \frac{g_s - g_D}{g_s + g_D}\beta$$
$$\leftrightarrow \beta = \frac{g_s + g_D}{2g_D}m$$
$$\leftrightarrow P' = -\frac{m}{4g_D}. \qquad (B15)$$

This implies that in the *CP* broken phase at $\theta = \pi$, the chiral $SU(2)$ symmetry is not spontaneously broken and the chiral order parameter does not evolve in T.

We come back to the case with arbitrary θ and derive relevant formulas for the susceptibilities χ_η and χ_{top} within the MFA. First, by noting the change of basis in Eq. (B6), the η susceptibility χ_η in χ_{top} of Eq. (4) is written in terms of the prime base as

$$\chi_\eta = \cos^2\frac{\theta}{2}\chi_\eta' - 2\sin\frac{\theta}{2}\cos\frac{\theta}{2}\chi_{\eta\sigma}' + \sin^2\frac{\theta}{2}\chi_\sigma', \qquad (B16)$$

The "primed" meson susceptibilities are evaluated in the so-called random phase approximation (the bubble-ring resummation ansatz) as

$$\mathbf{X}' = \mathbf{\Pi}' \cdot \frac{1}{\mathbf{1}_{2\times2} + \mathbf{G}' \cdot \mathbf{\Pi}'}, \qquad (B17)$$

where

$$\mathbf{X}' = \begin{pmatrix} \chi_\sigma' & \chi_{\eta\sigma}' \\ \chi_{\eta\sigma}' & \chi_\eta' \end{pmatrix},$$

$$\mathbf{\Pi}' = \begin{pmatrix} \Pi_\sigma' & \Pi_{\eta\sigma}' \\ \Pi_{\eta\sigma}' & \Pi_\eta' \end{pmatrix},$$

$$\mathbf{G}' = \begin{pmatrix} G_\sigma' & G_{\eta\sigma}' \\ G_{\eta\sigma}' & G_\eta' \end{pmatrix} = \begin{pmatrix} g_s + g_d & 0 \\ 0 & g_s - g_d \end{pmatrix}, \qquad (B18)$$

with the vacuum polarization functions for each channel,

$$\Pi_\sigma' = 2I_{S'},$$
$$\Pi_{\eta\sigma} = I_{S'P'},$$
$$\Pi_\eta' = 2I_{P'},$$
$$I_{S'} = -\frac{N_c}{\pi^2}\int_0^\Lambda dk k^2 \frac{E^2 - \alpha^2}{E^3}\left[1 - \frac{2}{e^{E/T} + 1}\right],$$
$$I_{S'P'} = \frac{N_c}{\pi^2}\int_0^\Lambda dk k^2 \frac{2\alpha\beta}{E^3}\left[1 - \frac{2}{e^{E/T} + 1}\right].$$
$$I_{P'} = -\frac{N_c}{\pi^2}\int_0^\Lambda dk k^2 \frac{E^2 - \beta^2}{E^3}\left[1 - \frac{2}{e^{E/T} + 1}\right]. \qquad (B19)$$

In evaluating the vacuum polarization functions, we have regularized the 3-momentum integrals by the cutoff Λ.

Putting all the relevant things above into χ_{top} in Eq. (4), we compute χ_{top} as a function of T and θ. The model parameter setting follows the literature [40,42,43]:

$$m = 6 \text{ MeV},$$

$$\Lambda = 590 \text{ MeV},$$

$$g_s = 2(1-c)G_0, \qquad g_d = 2cG_0 \quad \text{with} \quad G_0\Lambda^2 = 2.435 \quad \text{and} \quad c = 0.2. \tag{B20}$$

The g_d coupling has been related by c to the g_s coupling just in a numerical manner, though the associated asymmetry features are different.

See Fig. 3, where we observe several characteristic features: (i) the scalar condensate becomes dramatically smaller with increasing θ, so that χ_{top} in Eq. (4) gigantically decreases; (ii) at $\theta = \pi$, the pseudoscalar condensate undergoes the *CP* symmetry restoration of the second order type, which generates a significant spike at the criticality in χ_{top}; (iii) at $\theta = \pi$, the scalar condensate does not evolve in T at all until the *CP* symmetry is restored, in agreement with the analytic discussion around Eq. (B15).

2. PNJL case

By extending the NJL detailed in the previous subsection into the PNJL model in the MFA following the procedure in the literature [64] (for a recent review, see, e.g., [65]), we have the thermodynamic potential:

$$\Omega_{\text{PNJL}}[S', P', L, L^\dagger] = 2g_s(S'^2 + P'^2) + 2g_d(S'^2 - P'^2)$$

$$- 2N_f \int \frac{d^3k}{(2\pi)^3} \text{tr}_{\text{color}}[E + T(\ln(1 + L \cdot e^{-E/T}) + \text{H.c.})] + \mathcal{U}(L, L^\dagger)$$

$$= 2g_s(S'^2 + P'^2) + 2g_d(S'^2 - P'^2)$$

$$- 2N_c N_f \int \frac{d^3k}{(2\pi)^3} \left[E + \frac{T}{3}(\ln(1 + 3\Phi e^{-E/T} + 3\Phi^* e^{-2E/T} + e^{-3E/T}) + \text{H.c.}) \right] + \mathcal{U}(\Phi, \Phi^*), \tag{B21}$$

where $\Phi = \text{tr}[L]/3$, in which we have introduced the Polyakov loop field $L = \text{diag}\{e^{i\phi_1}, e^{i\phi_2}, e^{i\phi_3}\}$ with the Z_3 charges $\phi_{1,2,3}$; the $SU(3)$ constraint $\det[L] = 1$ taken into account; E takes the same form as in Eq. (B11), but would depend on the Polyakov-loop fields Φ and Φ^* through the stationary condition as in Eq. (B12). The Polyakov loop potential $\mathcal{U}(\Phi, \Phi^*)$ is assumed to take the form of polynomial type or logarithmic type:

$$\mathcal{U}_{\text{poly}}(\Phi, \Phi^*) = T^4 \left[-\frac{b_2(T)}{2}\Phi^*\Phi - \frac{b_3}{6}(\Phi^{*3} + \Phi^3) + \frac{b_4}{4}(\Phi^*\Phi)^2 \right],$$

$$\mathcal{U}_{\text{log}}(\Phi, \Phi^*) = T^4 \left[-\frac{c(T)}{2}\Phi^*\Phi + d(T) \ln(1 - 6\Phi\Phi^* + 4(\Phi^3 + \Phi^{*3}) - 3(\Phi\Phi^*)^2) \right], \tag{B22}$$

with

$$b_2(T) = a_0 + a_1\left(\frac{T_0}{T}\right) + a_2\left(\frac{T_0}{T}\right)^2 + a_3\left(\frac{T_0}{T}\right)^3,$$

$$c(T) = c_0 + c_1\left(\frac{T_0}{T}\right) + c_2\left(\frac{T_0}{T}\right)^2,$$

$$d(T) = d_3\left(\frac{T_0}{T}\right)^3. \tag{B23}$$

The Polyakov-loop potential parameters are fixed by fitting the lattice data in the pure Yang-Mills theory as [91,92]

a_0	a_1	a_2	a_3	b_3	b_4	c_0	c_1	c_2	d_3	T_0[MeV]
6.75	−1.95	2.625	−7.44	0.75	7.5	3.51	−2.47	15.2	−1.75	270

$$(B24)$$

The thermodynamic potential in Eq. (B21) is thus minimized also with respect to Φ and Φ^*, in addition to the stationary condition along S' and P' directions as in the NJL case, Eq. (B20).

In the RPA the following replacement rule for $I_{P'}$ in Eq. (B19) due to the Polyakov-loop contribution is applied:

$$I_{P'} \to I_{P'}(\Phi) = -\frac{N_c}{\pi^2}\int_0^\Lambda dk k^2 \frac{E^2 - \beta^2}{E^3}\left[1 - \left(\frac{e^{-E/T}(\Phi + 2\Phi^* e^{-E/T} + e^{-2E/T})}{1 + 3\Phi e^{-E/T} + 3\Phi^* e^{-2E/T} + e^{-3E/T}} + \text{H.c.}\right)\right]. \qquad (B25)$$

Similarly for $I_{S'}$ an $I_{S'P'}$ in Eq. (B19), we have

$$I_{S'} \to I_{S'}(\Phi) = -\frac{N_c}{\pi^2}\int_0^\Lambda dk k^2 \frac{E^2 - \alpha^2}{E^3}\left[1 - \left(\frac{e^{-E/T}(\Phi + 2\Phi^* e^{-E/T} + e^{-2E/T})}{1 + 3\Phi e^{-E/T} + 3\Phi^* e^{-2E/T} + e^{-3E/T}} + \text{H.c.}\right)\right],$$

$$I_{S'P'} \to I_{S'P'}(\Phi) = \frac{N_c}{\pi^2}\int_0^\Lambda dk k^2 \frac{2\alpha\beta}{E^3}\left[1 - \left(\frac{e^{-E/T}(\Phi + 2\Phi^* e^{-E/T} + e^{-2E/T})}{1 + 3\Phi e^{-E/T} + 3\Phi^* e^{-2E/T} + e^{-3E/T}} + \text{H.c.}\right)\right]. \qquad (B26)$$

Those modified integral functions are precisely reduced back to the ones in Eq. (B19) when $\Phi = 1$ (without confinement).

In Fig. 4 we plot the scalar and pseudoscalar condensates, $\langle\bar{q}q\rangle$ and $\langle\bar{q}i\gamma_5 q\rangle$, as a function of temperature T with $\theta/\pi = 0$, 0.5, 0.8, and 1. The scalar condensate decreases sharply with increasing θ. The pseudoscalar condensate undergoes a second-order phase transition at the critical temperature when $\theta = \pi$, and the *CP* symmetry is restored, which coincides with the NJL case (Fig. 3). At $\theta = \pi$, the scalar condensate does not evolve in T at all until the *CP* symmetry is restored at the critical temperature, in the same way as in the NJL case (Fig. 3) due to the same form of the gap equations as in
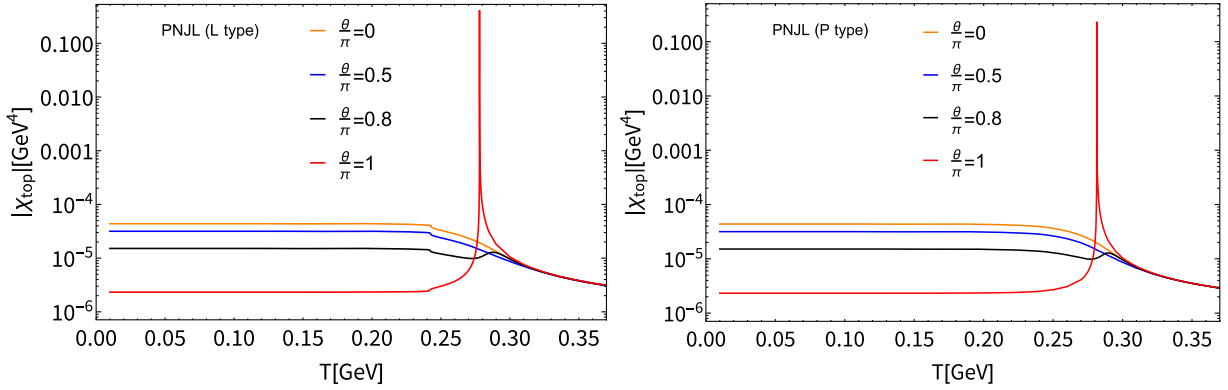

FIG. 5. Plot of χ_{top} (in magnitude) computed from the two-flavor PNJL model (with two types of PL potentials) with ranging θ from 0 to π as in Fig. 4.
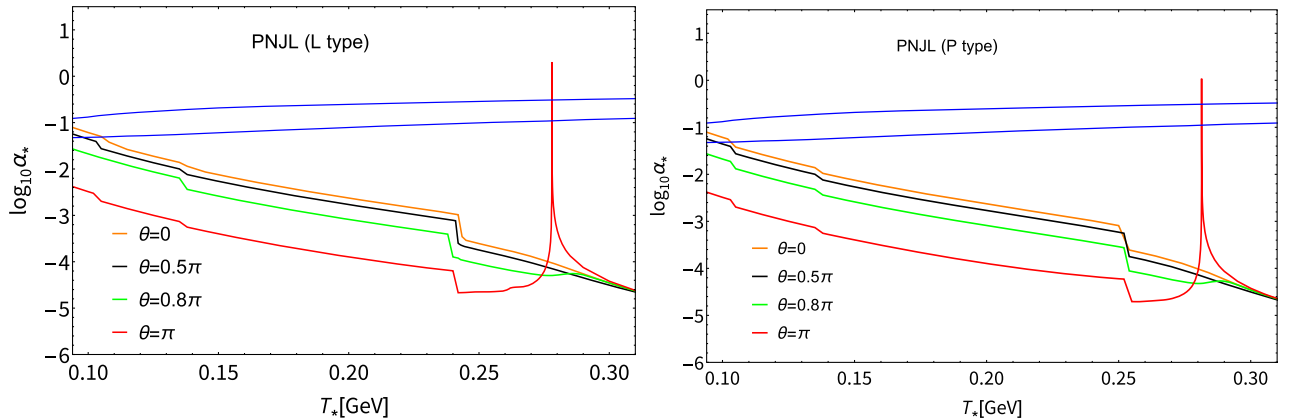

FIG. 6. The signal strength (the normalized latent heat) α_* versus T^* based on the formula in Eq. (13) with the two-flavor PNJL model estimate of χ_{top} and θ varied from 0 to π as in Figs. 4 and 5.

Eq. (B15) because incorporation of the Polyakov loop field does not break the $U(1)$ axial symmetry. This is the characteristic MFA feature, which persists both in the NJL and PNJL cases.

Those universal trends have also been seen in χ_{top}, in Fig. 5, which shows no substantial difference from the case of the NJL as in Fig. 1, hence the dramatic suppression of

α_* around $T = \mathcal{O}(100)$ MeV still persists for $\theta = \mathcal{O}(1)$ even with the PL contribution taken into account (See Fig. 6). At $\theta = \pi$, the peak signal strengths in the PNJL model (whichever type L or P) deviates from the 2σ contour, as has also been observed in the NJL case (Fig. 2 in the main text).

[1] G. Agazie *et al.* (NANOGrav Collaboration), Astrophys. J. Lett. **951,** L8 (2023).

[2] G. Agazie *et al.* (NANOGrav Collaboration), Astrophys. J. Lett. **952,** L37 (2023).

[3] A. Afzal *et al.* (NANOGrav Collaboration), Astrophys. J. Lett. **951,** L11 (2023).

[4] J. Antoniadis *et al.* (EPTA Collaboration), Astron. Astrophys. **678,** A48 (2023).

[5] J. Antoniadis *et al.* (EPTA and InPTA Collaborations), Astron. Astrophys. **678,** A49 (2023).

[6] J. Antoniadis *et al.* (EPTA and InPTA Collaborations), Astron. Astrophys. **678,** A50 (2023).

[7] D. J. Reardon, A. Zic, R. M. Shannon, G. B. Hobbs, M. Bailes, V. Di Marco, A. Kapur, A. F. Rogers, E. Thrane, J. Askew *et al.*, Astrophys. J. Lett. **951,** L6 (2023).

[8] D. J. Reardon, A. Zic, R. M. Shannon, V. Di Marco, G. B. Hobbs, A. Kapur, M. E. Lower, R. Mandow, H. Middleton, M. T. Miles *et al.*, Astrophys. J. Lett. **951,** L7 (2023).

[9] H. Xu, S. Chen, Y. Guo, J. Jiang, B. Wang, J. Xu, Z. Xue, R. N. Caballero, J. Yuan, Y. Xu *et al.*, Res. Astron. Astrophys. **23,** 075024 (2023).

[10] H. J. Li and Y. F. Zhou, arXiv:2401.09138.

[11] J. Ellis, M. Fairbairn, G. Franciolini, G. Hütsi, A. Iovino, M. Lewicki, M. Raidal, J. Urrutia, V. Vaskonen, and H. Veermäe, Phys. Rev. D **109,** 023522 (2024).

[12] K. D. Lozanov, S. Pi, M. Sasaki, V. Takhistov, and A. Wang, arXiv:2310.03594.

[13] G. B. Gelmini and J. Hyman, Phys. Lett. B **848,** 138356 (2024).

[14] N. Kitajima, J. Lee, K. Murai, F. Takahashi, and W. Yin, Phys. Lett. B **851,** 138586 (2024).

[15] M. Geller, S. Ghosh, S. Lu, and Y. Tsai, Phys. Rev. D **109,** 063537 (2024).

[16] Y. Bai, T. K. Chen, and M. Korwar, J. High Energy Phys. 12 (2023) 194.

[17] S. Blasi, A. Mariotti, A. Rase, and A. Sevrin, J. High Energy Phys. 11 (2023) 169.

[18] S. Borsanyi, Z. Fodor, J. Guenther, K. H. Kampert, S. D. Katz, T. Kawanai, T. G. Kovacs, S. W. Mages, A. Pasztor, F. Pittler *et al.*, Nature (London) **539,** 69 (2016).

[19] N. S. Manton, Phys. Rev. D **28,** 2019 (1983).

[20] F. R. Klinkhamer and N. S. Manton, Phys. Rev. D **30,** 2212 (1984).

[21] D. Kharzeev and A. Zhitnitsky, Nucl. Phys. **A797,** 67 (2007).

[22] D. E. Kharzeev, L. D. McLerran, and H. J. Warringa, Nucl. Phys. **A803,** 227 (2008).

[23] K. Fukushima, D. E. Kharzeev, and H. J. Warringa, Phys. Rev. D **78,** 074033 (2008).

[24] L. D. McLerran, E. Mottola, and M. E. Shaposhnikov, Phys. Rev. D **43,** 2027 (1991).

[25] G. D. Moore, Phys. Lett. B **412,** 359 (1997).

[26] G. D. Moore and K. Rummukainen, Phys. Rev. D **61,** 105008 (2000).

[27] D. Bodeker, G. D. Moore, and K. Rummukainen, Phys. Rev. D **61,** 056003 (2000).

[28] A. A. Andrianov, V. A. Andrianov, D. Espriu, and X. Planells, Phys. Lett. B **710,** 230 (2012).

[29] A. A. Andrianov, D. Espriu, and X. Planells, Eur. Phys. J. C **73,** 2294 (2013).

[30] M. Kawaguchi, S. Matsuzaki, and A. Tomiya, Phys. Rev. D **103,** 054034 (2021).

[31] C. X. Cui, J. Y. Li, S. Matsuzaki, M. Kawaguchi, and A. Tomiya, Phys. Rev. D **105,** 114031 (2022).

[32] C. X. Cui, J. Y. Li, S. Matsuzaki, M. Kawaguchi, and A. Tomiya, Particles **7,** 237 (2024).

[33] H. Leutwyler and A. V. Smilga, Phys. Rev. D **46,** 5607 (1992).

[34] M. Kawaguchi, S. Matsuzaki, and A. Tomiya, Phys. Lett. B **813,** 136044 (2021).

[35] R. F. Dashen, Phys. Rev. D **3,** 1879 (1971).

[36] E. Witten, Ann. Phys. (N.Y.) **128,** 363 (1980).

[37] R. D. Pisarski, Phys. Rev. Lett. **76,** 3084 (1996).

[38] M. Creutz, Phys. Rev. Lett. **92,** 201601 (2004).

[39] A. J. Mizher and E. S. Fraga, Nucl. Phys. **A831,** 91 (2009).

[40] D. Boer and J. K. Boomsma, Phys. Rev. D **78,** 054027 (2008).

[41] M. Creutz, Ann. Phys. (Amsterdam) **324,** 1573 (2009).

[42] J. K. Boomsma and D. Boer, Phys. Rev. D **80,** 034019 (2009).

[43] Y. Sakai, H. Kouno, T. Sasaki, and M. Yahiro, Phys. Lett. B **705,** 349 (2011).

[44] B. Chatterjee, H. Mishra, and A. Mishra, Phys. Rev. D **85,** 114008 (2012).

[45] T. Sasaki, J. Takahashi, Y. Sakai, H. Kouno, and M. Yahiro, Phys. Rev. D **85,** 056009 (2012).

[46] T. Sasaki, H. Kouno, and M. Yahiro, Phys. Rev. D **87,** 056003 (2013).

[47] S. Aoki and M. Creutz, Phys. Rev. Lett. **112,** 141603 (2014).

[48] K. Mameda, Nucl. Phys. **B889,** 712 (2014).

[49] J. J. M. Verbaarschot and T. Wettig, Phys. Rev. D **90,** 116004 (2014).

[50] D. Gaiotto, Z. Komargodski, and N. Seiberg, J. High Energy Phys. 01 (2018) 110.

[51] D. Gaiotto, A. Kapustin, Z. Komargodski, and N. Seiberg, J. High Energy Phys. 05 (2017) 091.

[52] G. 't Hooft, NATO Sci. Ser. B **59,** 135 (1980).

[53] Y. Frishman, A. Schwimmer, T. Banks, and S. Yankielowicz, Nucl. Phys. **B177,** 157 (1981).

[54] K. Saikawa, Universe **3,** 40 (2017).

[55] T. Hiramatsu, M. Kawasaki, and K. Saikawa, J. Cosmol. Astropart. Phys. 05 (2010) 032.

[56] T. Hiramatsu, M. Kawasaki, K. Saikawa, and T. Sekiguchi, J. Cosmol. Astropart. Phys. 01 (2013) 001.

[57] T. Hiramatsu, M. Kawasaki, and K. Saikawa, J. Cosmol. Astropart. Phys. 02 (2014) 031.

[58] R. L. Workman *et al.* (Particle Data Group), Prog. Theor. Exp. Phys. **2022,** 083C01 (2022).

[59] Y. Aoki, S. Borsanyi, S. Durr, Z. Fodor, S. D. Katz, S. Krieg, and K. K. Szabo, J. High Energy Phys. 06 (2009) 088.

[60] S. Borsanyi, G. Endrodi, Z. Fodor, C. Hoelbling, S. Katz, S. Krieg, C. Ratti, and K. Szabo (Wuppertal-Budapest Collaboration), J. Phys. Conf. Ser. **316,** 012020 (2011).

[61] H. T. Ding, F. Karsch, and S. Mukherjee, Int. J. Mod. Phys. E **24,** 1530007 (2015).

[62] A. Bazavov *et al.* (HotQCD Collaboration), Phys. Lett. B **795,** 15 (2019).

[63] H. T. Ding, Nucl. Phys. **A1005,** 121940 (2021).

[64] K. Fukushima, Phys. Lett. B **591,** 277 (2004).

[65] K. Fukushima and V. Skokov, Prog. Part. Nucl. Phys. **96,** 154 (2017).

[66] M. Ruggieri, M. N. Chernodub, and Z. Y. Lu, Phys. Rev. D **102,** 014031 (2020).

[67] S. Chen, K. Fukushima, H. Nishimura, and Y. Tanizaki, Phys. Rev. D **102,** 034020 (2020).

[68] M. Kobayashi and T. Maskawa, Prog. Theor. Phys. **44,** 1422 (1970).

[69] M. Kobayashi, H. Kondo, and T. Maskawa, Prog. Theor. Phys. **45,** 1955 (1971).

[70] G. 't Hooft, Phys. Rev. Lett. **37,** 8 (1976).

[71] G. 't Hooft, Phys. Rev. D **14,** 3432 (1976); **18,** 2199(E) (1978).

[72] G. Fejos and A. Hosaka, Phys. Rev. D **94,** 036005 (2016).

[73] G. Fejos and A. Patkos, Phys. Rev. D **109,** 036035 (2024).

[74] G. Fejös and A. Patkos, Phys. Rev. D **105,** 096007 (2022).

[75] L. Del Debbio, H. Panagopoulos, and E. Vicari, J. High Energy Phys. 08 (2002) 044.

[76] M. D'Elia, Nucl. Phys. **B661,** 139 (2003).

[77] L. Del Debbio, G. M. Manca, H. Panagopoulos, A. Skouroupathis, and E. Vicari, Proc. Sci. LAT2006 (**2006**) 045 [arXiv:hep-th/0610100].

[78] L. Giusti, S. Petrarca, and B. Taglienti, Phys. Rev. D **76,** 094510 (2007).

[79] T. Izubuchi, S. Aoki, K. Hashimoto, Y. Nakamura, T. Sekido, and G. Schierholz, Proc. Sci. LATTICE2007 (**2007**) 106 [arXiv:0802.1470].

[80] E. Vicari and H. Panagopoulos, Phys. Rep. **470,** 93 (2009).

[81] M. D'Elia and F. Negro, Phys. Rev. D **88,** 034503 (2013).

[82] M. Hirasawa, K. Hatakeyama, M. Honda, A. Matsumoto, J. Nishimura, and A. Yosprakob, Proc. Sci. LATTICE2023 (**2024**) 193 [arXiv:2401.05726].

[83] R. Kitano, R. Matsudo, N. Yamada, and M. Yamazaki, Phys. Lett. B **822,** 136657 (2021).

[84] T. Byrnes, P. Sriganesh, R. J. Bursill, and C. J. Hamer, Nucl. Phys. B, Proc. Suppl. **109,** 202 (2002).

[85] L. Funcke, K. Jansen, and S. Kühn, Phys. Rev. D **101,** 054507 (2020).

[86] Y. Kuramashi and Y. Yoshimura, J. High Energy Phys. 04 (2020) 089.

[87] B. Chakraborty, M. Honda, T. Izubuchi, Y. Kikuchi, and A. Tomiya, Phys. Rev. D **105,** 094503 (2022).

[88] M. Honda, E. Itou, Y. Kikuchi, L. Nagano, and T. Okuda, Phys. Rev. D **105,** 014504 (2022).

[89] M. Honda, *Proceedings of the East Asia Joint Symposium on Fields and Strings 2021* (World Scientific, Singapore, 2022).

[90] A. Gómez Nicola and J. Ruiz de Elvira, J. High Energy Phys. 03 (2016) 186.

[91] S. Roessner, C. Ratti, and W. Weise, Phys. Rev. D **75,** 034007 (2007).

[92] C. Ratti, M. A. Thaler, and W. Weise, Phys. Rev. D **73,** 014019 (2006).